Applied Mathematics & Information Sciences
An International Journal

http://dx.doi.org/10.18576/amis/130609

Analysis of TiO_2–ZnO/EG Hybrid Nanofluid Effect on Heat Transfer Enhancement

D. Nesakumar[1,*] *and R. Baskar*[2]

[1] Department of Chemical Engineering, Kongu Engineering College, Perundurai, Erode, Tamilnadu, India
[2] Department of Food Technology, Kongu Engineering College, Perundurai, Erode, Tamilnadu, India

Received: 2 Mar. 2019, Revised: 12 May 2019, Accepted: 20 May 2019
Published online: 1 Nov. 2019

Abstract: We employ 2^3 full factorial design to analyze the effect of temperature, volume fraction of hybrid nanofluids and channel height on heat transfer intensification through microchannel under laminar conditions. The range of temperature is varied from 30 °C to 50 °C and the volume fractions of hybrid nanoparticles TiO_2/ZnO in ethylene glycol are varied from 1% to 4% and the channel height is varied from 200 μm to 400 μm. Using MINITAB 18 software, experiments were conducted with 24 runs using TiO_2–ZnO/Ethylene glycol hybrid nanofluids in the rectangular microchannel heat exchanger. Based on this experimental study, various numerical simulations have been discussed and the applications of variance analysis, the effects of the different parameters on Nusselt number have been analyzed. The test results depict that all the three parameters have a significant effect on the thermal conductivity of TiO_2–ZnO/ethylene glycol hybrid nanofluids, which enhances the Nusselt number as well as the heat transfer in the microchannel heat exchanger. The results show that maximum Nusselt number is obtained at higher temperature, volume fraction and microchannel.

Keywords: factorial design; hybrid nanofluids; thermal conductivity; Nusselt number

1 Introduction

Usage of microchannels is one of the best techniques for cooling semiconductor electronic devices which transfer more heat flux at reliable surface temperature. Microchannel has many advantages, including compact design, better heat transfer and less weight. Dispersion of nano-sized particles in the base fluid enhances the thermal properties and heat transfer rate. The usage of microchannel and hybrid nanofluids to enhance the rate of heat transfer has gained an increasing research interest recently. Mohammed et al., studied the effect of microchannel configuration on heat transfer rate and it was found that the performance of wavy microchannel is better than that of straight microchannel [1]. Tu–Chieh Hung et al., suggested that the selection of proper volume fraction of Al_2O_3 nanoparticles in a base fluid (water) has enhanced the heat transfer process [2]. Manikandan et al., studied the individual and combined influence of temperature, nanofluid concentration and flow rate on thermal conductivity of nanofluid using analysis of variance [3]. Mark et al., investigated the applicability of heat intensification methods for mini and microchannels under single phase flow [4]. Chai et al., experimentally investigated the enhancement of heat transfer in microchannel by varying the cross sections [5]. Akbarinia et al., found that the increase in the velocity of the nanofluid and the volume fraction of nanoparticles enhance the Nusselt number. [6].

Chein et al., found that variations in microchannel dimensions and the flow of nanofluids effectively enhance its cooling performance [7]. Ho et al., analyzed the performance of copper minichannel by varying the Reynolds number and the heating power with Al_2O_3 nanoparticles in water [8]. Tahir et al., statistically analyzed the impact of Reynolds number, volume fraction and particle size on heat transfer coefficient using factorial design [9]. Kwang-Yong et al., numerically optimized the channel dimensions for effective heat transfer by turbulence using factorial designs [10]. Afzal et al., numerically optimized Micro Channel Heat Sink by choosing various microchannel dimensions like width and depth by evolutionary algorithms [11]. Mamourian et al., estimated the optimum conditions for convective heat transfer in square cavity wavy surface using Taguchi method by flowing Cu–water nanofluid [12].

* Corresponding author e-mail: nesakumar2006@gmail.com

Suresh et al., found that usage of Al_2O_3–Cu/water hybrid nanofluid in a circular tube significantly increases the Nusselt number more than pure water under laminar conditions [13]. Syam Sundar et al., estimated the effect of hybrid nanofluids on friction factor flowing through a circular tube [14]. Madhesh et al., investigated the influence of copper–titania hybrid nanofluids (HyNF) on Nusselt number in counter current tube type heat exchanger [15]. Afrand et al., experimentally investigated the temperature and volume fraction of nanocomposite powder influence on physical properties of Fe_3O_4–Ag nanocomposite in ethylene glycol [16]. Esfe et al., investigated the interactive effect of temperature and volume fraction on thermal conductivity of hybrid nanofluids and optimized the thermal and rheological properties of Al_2O_3–ethylene glycol/water nanofluid by using Response Surface Methodology (RSM) [17]. Maddah et al., statistically analyzed the thermal performance of double pipe heat exchanger using Al_2O_3–TiO_2 by factorial experimental design and found that usage of hybrid nanofluids as a service fluid yields more heat transfer than the conventional water [18].

Many research works focusing on heat transfer applications with nanocomposite powder dispersed in a base fluid have been found in the literature. But there is no much work carried out to identify the influence of various independent variables on Nusselt number enhancement and heat transfer enhancement through microchannel under laminar conditions by factorial design analysis. Also, many research works are estimate the influence of fluid temperature, volume fraction of solid particles and mass flow rate of fluid on Nusselt number. Only a few works were carried out to study the impact of microchannel height on Nusselt number. For this reason, this paper focuses on the effects of fluid inlet temperature, volume fraction and microchannel height on Nusselt number.

This work is mainly based on the application of the principles of the 24-run factorial designs with consideration of the independent variables like temperature, volume fraction of hybrid nanoparticles and microchannel height on Nusselt number. Also the individual and combined effects of these independent variables on Nusselt number are analyzed. Based on this experimental study, Normal, Pareto, Residual plots for Nusselt number, Interval plot of Nusselt number vs all independent variables, Main and Interaction effects, contour plot and surface plot are obtained. Also by variance analysis, the effects of the above three parameters on Nusselt number are analyzed.

2 Design and Analysis of Experiment

2.1 Experimentation method

Experimental setup consists of a control unit to control the fluid flow and measuring and testing units to measure and test the response for the given inputs. In flow control unit, 0–6 litres is the volumetric flow rate of fluid which is achieved by a positive displacement pump. An inverter connected with the pump is employed to maintain the working fluid volumetric flow rate. The accuracy of the flow rate is about $\pm 0.05\%$. Similarly, a temperature bath is used to confirm that the inlet temperature of the fluid enters into the testing channel. To avoid the vibrational effect, the mass flow meter is connected with a flexible pipe. To estimate the effect of microchannel height on heat transfer intensification, three gauges with heights of 200 μm, 300 μm and 400 μm are used. The plates are made up of bronze due to its high thermal conductivity. Thermocouples are employed to measure the temperature of the exit fluid and pressure transducer is used to measure the pressure drop in the microchannel. The inlet and outlet temperature of the fluids are measured with the help of T-type thermocouples. The inlet temperature of the fluid can be adjusted by applying the heat flux with the help of a variable transformer. All measured temperatures were recorded after the attainment of thermal equilibrium which is normally obtained within 35–40 minutes. After recording the first set of readings by using the recorder, the flow rate of the fluid was set to the next value and the experiment was repeated. The variation in the fluid outlet temperature for different volume fraction of hybrid nanofluid, different microchannel height and the variation in fluid inlet temperature are measured and recorded in the recorder. Based on the measured outlet temperature of the fluid, the Nusselt number is estimated by using equation (7). Fig. 1 illustrates the experimental setup.

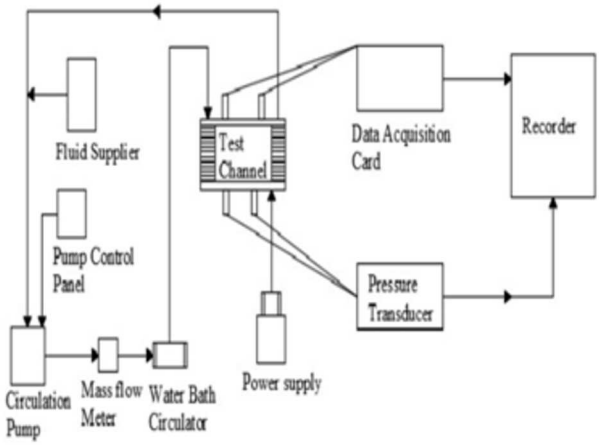

Fig. 1: Experimental setup

2.2 Determination of thermo physical properties

The volume fraction of hybrid nanoparticles is estimated by using the following equation: [19]

$$\phi\% = \frac{\omega\rho_{bf}}{\left(\frac{\omega}{100}\right)\rho_{bf} + \left(1-\frac{\omega}{100}\right)\rho_p} \times 100 \tag{1}$$

where φ, ω and ρ are volume concentration, weight concentration and density respectively.

Dispersing nanocomposite powder in a base fluid greatly influences the thermal properties of the hybrid nanofluid [20]. The effective properties of composite nanofluid, according to Tayebi and Chamkha [21], Pak and Cho [22], Xuan and Roetzel [23] are:

$$\rho_{hnf} = (1-\varphi)\rho_f + \varphi\rho_{hp} \tag{2}$$

$$C_{p_{hnf}} = (1-\varphi)(C_p)_f + \varphi(C_p)_{hp} \tag{3}$$

Based on the model proposed by Patel et al., the thermal conductivity is measured by: [24]

$$\frac{k_{nf}-k_{bf}}{k_{bf}} = \frac{k_p}{k_{bf}}\left(1 + c\frac{u_{pd_p}}{\alpha_{bf}}\right)\frac{d_{bf}}{d_p}\frac{\varphi}{1-\varphi} \tag{4}$$

The thermophysical properties of the prepared composite nanofluids are calculated at their average temperature.

Procedure for estimation of the heat transfer coefficient and Nusselt number is given in detail. The heat energy absorbed by the fluid through the heaters is given by the equations [25, 26]

$$Q = V^2R = VI = mC_p(T_{out} - T_{in}) = Q_{con}. \tag{5}$$

After estimating the Q_{con} by Eq. (5), the convective heat transfer coefficient is estimated [25,26] as given in Eq: (6).

$$h = \frac{Q_{con}}{A \times (T_s - T_{avg})}. \tag{6}$$

where A is the area of the channel available for convection.

The Nusselt number is calculated as below, according to Sieder and Tate [27]:

$$Nu = \frac{hD_h}{k_f} = \frac{Q_{con}D_h}{A\,(T_S - T_{avg})\,k_f}. \tag{7}$$

where D_h is the hydraulic diameter of the channel.

With the help of MINITAB 18 factorial design of experiments, the experiments are conducted with different combinations of input parameters and the properties of the hybrid nanofluids are estimated by using Eqs. (1) to (4). Similarly, the heat transfer rate, convective heat transfer coefficient and Nusselt number are estimated by using Eqs. (5), (6) and (7) respectively.

Table 1: Variables and range of levels for full factorial design

Variable selected	Unit	Level	
		Low (−1)	High (+1)
Fluid Temperature (T)	°C	30	50
Solid Volume Fraction (ϕ)	–	1%	4%
Channel Height (H)	μm	200	400

2.3 Experimentation procedure: Levels of Input parameters

In this study, two-level three factors full factorial design with three replications is used to examine the foremost and combined effects of independent variables on the increase in the Nusselt number by flowing TiO_2–ZnO/ethylene glycol hybrid nanofluids through microchannels with different height. The full factorial design will build an experiment which includes every probable combination of factor levels [28]. Two-level factorial designs were carried out to form probable curvature in the response function (Nusselt number). The experiments were arbitrarily consigned in two blocks to allocate unpredicted inaccuracies. The influence of fluid inlet temperature (T), nanocomposite powder volume fraction (ϕ), microchannel height and their shared interactions and the curvature effect of these parameters on Nusselt number were checked by the analysis of variance using MINITAB 18 software and base design 3, 8.

In this work, the critical P-value was considered as 0.05. To check the impact of the independent variables on the Nusselt number, the values of critical P and attained P were analyzed. Each estimated parameter examined with 2 levels, namely high $(+1)$ and low (-1) and the corresponding maximum and minimum values of these parameters were given in Table 1. 24 trial runs were intended to analyze the significance of the individual and the interactive effects of parameters on Nusselt number. Table 2 exhibits the design layout, standard order, runs order, independent variable values and corresponding response factor results of 2^3 full factorial design and Table 3 gives the final factorial design summary.

The observed Nusselt number values through microchannel under the usage of TiO_2–ZnO/ethylene glycol hybrid nanofluid were compared with those under the usage of base fluids like pure water and pure ethylene glycol through microchannel. From previous work, it was found that the Nusselt number increases when hybrid nanofluids are applied for heat transfer process [29]. Similarly, an increase in Nusselt number due to an increase in different parameters like temperature, volume fraction of hybrid nanoparticles and microchannel height was also observed. By the experimental work, it is observed that TiO_2–ZnO/ethylene glycol hybrid nanofluid give a better enhancement in Nusselt number than TiO_2–ZnO/water hybrid nanofluid and this is because of

Table 2: Experiment results of 24 factorial design

Standard Order	Run Order	Center Point	Blocks	Temp. (°C)	Vol. frac.	Ch. height (μm)	Nusselt number
4	1	1	1	30	4	400	14.6
3	2	1	1	50	1	400	29.3
10	3	1	1	50	4	200	29.8
9	4	1	1	30	1	200	10.2
7	5	1	1	50	1	400	29.5
6	6	1	1	50	4	200	30
8	7	1	1	30	4	400	14.5
5	8	1	1	30	1	200	10.4
2	9	1	1	50	4	200	29.8
11	10	1	1	50	1	400	29.5
12	11	1	1	30	4	400	14.5
1	12	1	1	30	1	200	10.3
19	13	1	2	30	1	400	13.3
16	14	1	2	50	4	400	31.6
17	15	1	2	50	1	200	28.8
18	16	1	2	30	4	200	12.8
21	17	1	2	50	1	200	28.8
22	18	1	2	30	4	200	13
15	19	1	2	30	1	400	13.5
13	20	1	2	50	1	200	28.9
23	21	1	2	30	1	400	13.5
24	22	1	2	50	4	400	31.8
20	23	1	2	50	4	400	31.5
14	24	1	2	30	4	200	12.8

Table 3: Design summary

No. of Variables	3
Basic design	3, 8
Total number of runs	24
No. of Replicates	3
No. of Blocks	2

the superior thermophysical properties of TiO_2–ZnO/ethylene glycol hybrid nanofluid.

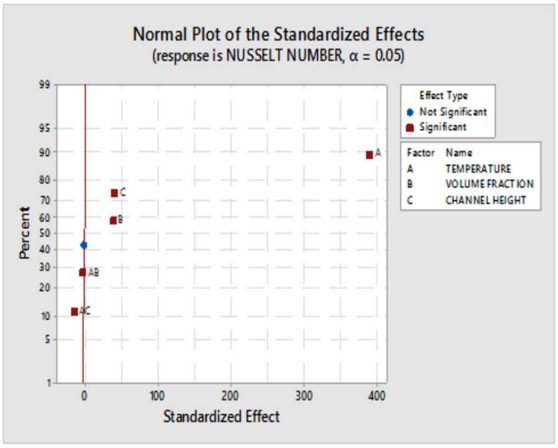

(a) Standardized effects for Nusselt number due to TiO_2–ZnO/EG hybrid nanofluid

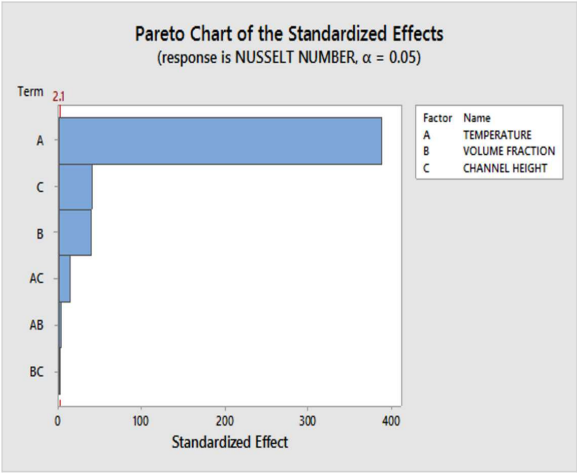

(b) Standardized effects for Nusselt number due to TiO_2–ZnO/EG hybrid nanofluid using Pareto Chart

Fig. 2

3 Results and Discussions

3.1 Standard results on Nusselt number due to TiO_2–ZnO/ethylene glycol hybrid nanofluid by Normal and Pareto Chart

Normal probability plot is used to find the magnitude, direction and the significance of the effects [30]. Primarily on this normal plot, effects that are further from 0 are statistically considerable. From Fig. 2(a), the main effects of factors like temperature, volume fraction and channel height are statistically important at the 5% level. A Pareto Chart is used to find the magnitude and the significance of the effects [31]. In any Pareto chart, bars that extends further than the reference line are statistically considerable. From this Pareto chart, Fig. 2(b), the bars that correspond to factors A, B, C, AC and AB exceed the reference line that is at 2.1. These individual and combined factors are statistically very important at the 5% level with the current model. From these two plots, it is observed that A, B, C, AC (combination of A and C) and AB (combination of A and B) are very important, i.e., the parameters temperature (A), volume fraction of hybrid nanoparticles (B), channel height (C), interaction of AB and AC are significant [32].

It is also observed from the normal plot that the interaction of AB and AC has a close-to-negative standardized effect while that of A, B, C has positive standardized effects. Among these three independent factors, temperature has a more considerable effect on the Nusselt number (response factor) and B and C have similar effects on Nusselt number (response factor). This observation is similar to the observations reported for Nusselt number enhancement (Madhesh et al.,) [15].

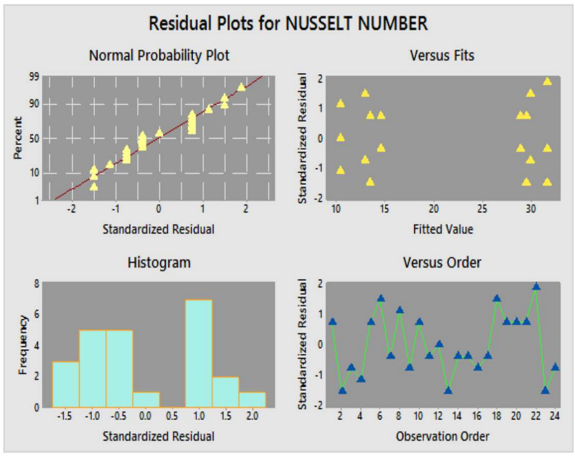

Fig. 3: Residual plots for Nusselt number

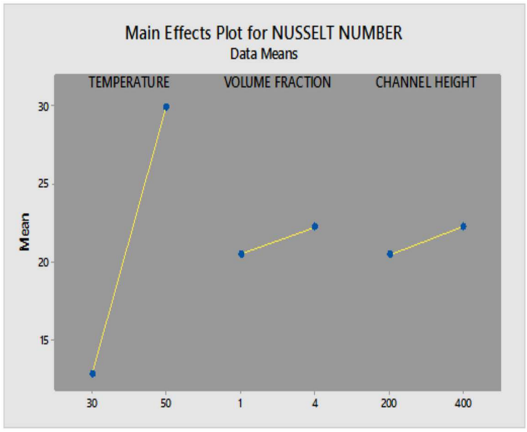

(a) Main effects plot for Nusselt number

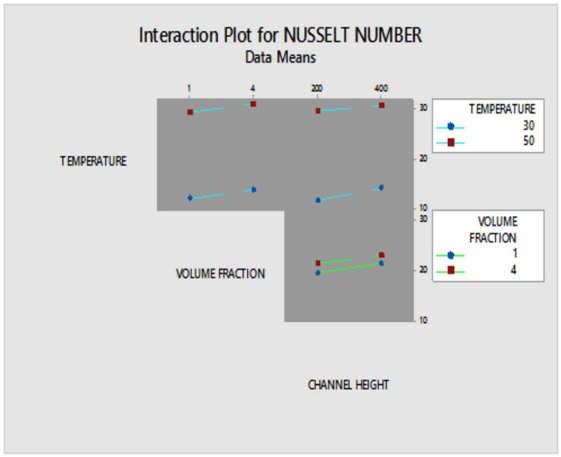

(b) Interaction plot for Nusselt number

Fig. 4

3.2 Residual Plots for Nusselt number

Fig. 3 illustrates the residual plots for Nusselt number which validate the other assumptions [33]. Normal probability plot shows that the residuals points form a straight line and indicates that the residuals are distributed which also validate the assumptions [34]. Residual versus fitted values plot shows that there could be a non-linear relationship between the predictor variables and outcome variables which confirms the constant variance assumption. The residual histogram is normally used to know the distribution of error terms [34] and the plot between the residual and the order generally propose the relationship between the error terms.

3.3 Analysis of ANOVA

Analysis of variance on the Nusselt number were applied to verify the consequence of the replica [35]. Table 4 explains the numerical consequences of the Nusselt number obtained using ANOVA and Table 5 shows the model summary.

From the model summary, the obtained value of R^2 is nearer to 1 which shows a better model [36]. The R^2 obtained during this experiment was 0.9999 which proves that this model may well suit for over 0.9999. From the summary, the value of the adjusted R^2 was very high (0.9999), which confirms that the model is significant to a great extent [37]. Similarly, the value of R^2 and the adjusted R^2 are very nearer to each other which confirms that this replica could not contain any trivial variables [38].

3.4 Effects of variable factors

Table 4 (ANOVA) sums up the individual and interactive impacts of fluid temperature, solid volume fraction and channel height on the Nusselt number (response factor). Variation in the mean response indicates the happening of a key effect. The main effects plots obtained by this analysis are used to investigate the comparative strength of effects. Fig. 4(a) shows the major effect of fluid temperature, nanocomposite powder volume fraction and height of channel on the Nusselt number and Fig. 4(b) explains the interaction effects of temperature, nanocomposite powder volume fraction and channel height on Nusselt number in microchannel by flowing TiO_2–ZnO/ethylene glycol hybrid nanofluids [13].

3.5 Regression Equation

The purpose of this work is to examine the individual and combined effects of independent parameters, temperature, volume fraction and microchannel height on increase in Nusselt number through microchannel. Based on the full factorial design, the final statistical relationship between Nusselt number and the variable factors: temperature (A),

Table 4: Analysis of variance

Source	DF	Adjusted SS	Adjusted MS	F-Value	P-Value	Significance
Model	7	1808.49	258.36	22144.77	0.000	Significant
Blocks	1	2.60	2.60	222.89	0.000	Significant
Linear	3	1803.56	601.19	51530.42	0.000	Significant
Temperature	1	1766.45	1766.45	151410.04	0.000	Significant
Volume fraction	1	17.85	17.85	1530.32	0.000	Significant
Channel Height	1	19.26	19.26	1650.89	0.000	Significant
Two Way Interactions	3	2.32	0.77	66.42	0.000	Significant
Temperature* Volume fraction	1	0.07	0.07	6.04	0.026	Significant
Temperature* Channel Height	1	2.22	2.22	190.32	0.000	Significant
Volume fraction* Channel Height	1	0.03	0.03	2.89	0.108	Not significant
Error	16	0.19	0.01			
Total	23	1808.68				

Table 5: Summary of the model

S	R^2	R^2(adjusted)	R^2(predicted)
0.108012	0.9999	0.9999	0.9998

volume fraction (B) and microchannel height (C) is given as below:

$$Nu = -21.278 + 0.95819A + 0.7944B + 0.021750C - 0.00361AB - 0.000304AC - 0.000250BC \quad (8)$$

3.6 Contour Plot and Surface plot

From the contour plot, it has been noticed that the maximum Nusselt number is obtained for higher temperature and higher volume fraction of hybrid nanoparticles. From this plot, it has been also noticed that Nu is increased from bottom to top and the area at the extreme right corner indicates a higher Nusselt number. Fig. 5 illustrates the interaction consequence of fluid temperature and nanocomposite fraction on Nu and it has been observed that by increasing temperature and volume fraction, the Nusselt number has an increasing pattern [16]. Fig. 6 gives the surface plot of Nusselt number versus temperature and volume fraction which indicates that the change in Nusselt number is directly proportional to fluid temperature and solid volume fraction. This result is similar to that obtained in a previous study (Suresh et al.,) [13].

4 Conclusion

In this research work, Nusselt number changes under the TiO_2–ZnO/ethylene glycol hybrid nanofluid flow through microchannel were examined by 24 runs full factorial design with the help of MINITAB 18 software. To analyze the enhancement in Nusselt number due to the independent variables like temperature, volume fraction and microchannel height, three factors with two-level effects were considered. 30 °C and 50 °C, 1% and 4% and

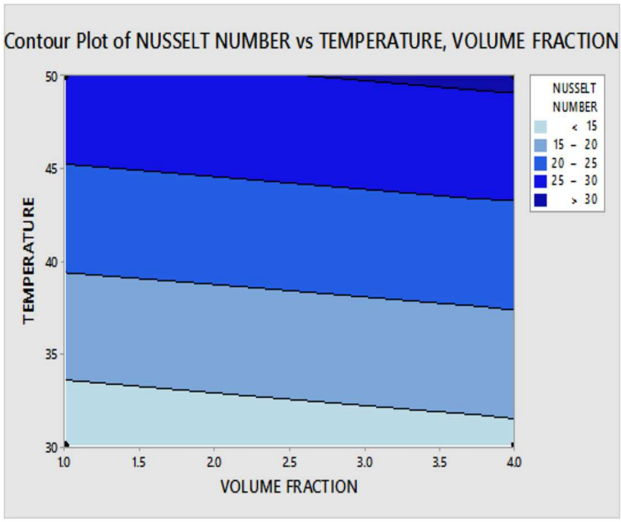

Fig. 5: Contour plot for Nusselt number (Nu vs. T & ϕ)

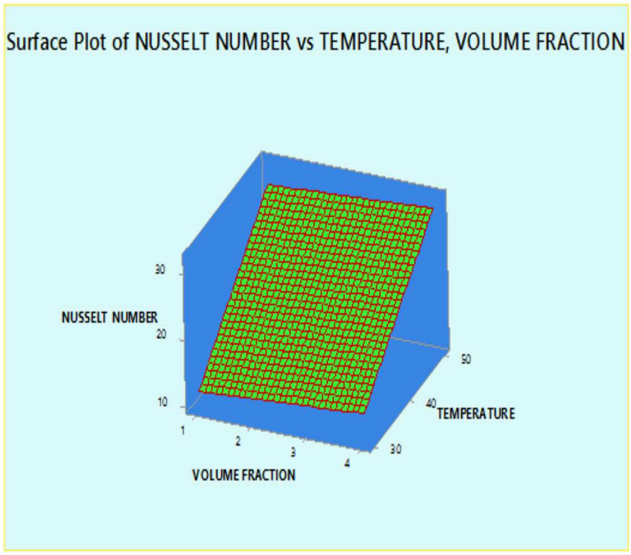

Fig. 6: Surface plot of Nusselt number (Nu vs. T &ϕ)

200 μm and 400 μm were considered for temperature, volume fraction and microchannel height respectively. Full factorial design was used to identify the significant factor among the three independent variables. From the various plots obtained from the full factorial design and the analysis of variance (ANOVA) table, it was observed that three independent variables having significant effects on Nusselt number. Similarly, it is also found that the combination of temperature and volume fraction, temperature and microchannel height has a major effect on Nu, whereas interaction of volume fraction and microchannel height have no much significant effect on Nusselt number. Various plots like main effects and interaction plots, normal and Pareto chart, residual plots, contour and surface plot were obtained with Nusselt number as a response factor. The maximum Nusselt number of 31.8 for TiO_2–ZnO/ethylene glycol hybrid nanofluid through microchannel was attained at T = 50 °C, $\phi = 4\%$ and H = 400 μm where T, ϕ and H represents fluid temperature, solid volume fraction and microchannel height respectively.

References

[1] H. Mohammed, P. Gunnasegaran and N. Shuaib, Numerical simulation of heat transfer enhancement in wavy microchannel heat sink. International Communications in Heat and Mass Transfer, **38**(1), 63–68 (2011).

[2] T.-C. Hung, W.-M. Yan, X.-D. Wang and C.-Y. Chang, Heat transfer enhancement in microchannel heat sinks using nanofluids. International Journal of Heat and Mass Transfer, **55**(9–10), 2559–2570 (2012).

[3] S.M. Periasamy and R. Baskar, Assessment of the Influence of Graphene Nanoparticles on Thermal Conductivity of Graphene/water Nanofluids Using Factorial Design of Experiments. Periodica Polytechnica Chemical Engineering, **62**(3), 317–322 (2018).

[4] M.E. Steinke and S.G. Kandlikar, Single-phase heat transfer enhancement techniques in microchannel and minichannel flows. In, ASME 2004 2nd International Conference on Microchannels and Minichannels, American Society of Mechanical Engineers, 141–148 (2004).

[5] L. Chai, G. Xia, L. Wang, M. Zhou and Z. Cui, Heat transfer enhancement in microchannel heat sinks with periodic expansion–constriction cross-sections. International Journal of Heat and Mass Transfer, **62**, 741–751 (2013).

[6] A. Akbarinia, M. Abdolzadeh and R. Laur, Critical investigation of heat transfer enhancement using nanofluids in microchannels with slip and non-slip flow regimes. Applied Thermal Engineering, **31**(4), 556–565 (2011).

[7] R. Chein and G. Huang, Analysis of microchannel heat sink performance using nanofluids. Applied thermal engineering, **25**(17–18), 3104–3114 (2005).

[8] C.-J. Ho, L. Wei and Z. Li, An experimental investigation of forced convective cooling performance of a microchannel heat sink with Al_2O_3/water nanofluid. Applied Thermal Engineering, **30**(2–3), 96–103 (2010).

[9] S. Tahir and M. Mital, Numerical investigation of laminar nanofluid developing flow and heat transfer in a circular channel. Applied Thermal Engineering, **39**, 8–14 (2012).

[10] K.-Y. Kim and J.-Y. Choi, Shape optimization of a dimpled channel to enhance turbulent heat transfer. Numerical Heat Transfer, Part A, Applications, **48**(9), 901–915 (2005).

[11] A. Husain and K.-Y. Kim, Optimization of a microchannel heat sink with temperature dependent fluid properties. Applied thermal engineering, **28**(8–9), 1101–1107 (2008).

[12] M. Mamourian, K.M. Shirvan, R. Ellahi and A. Rahimi, Optimization of mixed convection heat transfer with entropy generation in a wavy surface square lid-driven cavity by means of Taguchi approach. International Journal of Heat and Mass Transfer, **102**, 544–554 (2016).

[13] S. Suresh, K. Venkitaraj, P. Selvakumar and M. Chandrasekar, Effect of Al_2O_3–Cu/water hybrid nanofluid in heat transfer. Experimental Thermal and Fluid Science, **38**, 54–60 (2012).

[14] L.S. Sundar, M.K. Singh and A.C. Sousa, Enhanced heat transfer and friction factor of MWCNT–Fe_3O_4/water hybrid nanofluids. International Communications in Heat and Mass Transfer, **52**, 73–83 (2014).

[15] D. Madhesh, R. Parameshwaran and S. Kalaiselvam, Experimental investigation on convective heat transfer and rheological characteristics of Cu–TiO_2 hybrid nanofluids. Experimental Thermal and Fluid Science, **52**, 104–115 (2014).

[16] M. Afrand, D. Toghraie and B. Ruhani, Effects of temperature and nanoparticles concentration on rheological behavior of Fe_3O_4–Ag/EG hybrid nanofluid, an experimental study. Experimental Thermal and Fluid Science, **77**, 38–44 (2016).

[17] M.H. Esfe, M. Firouzi, H. Rostamian and M. Afrand, Prediction and optimization of thermophysical properties of stabilized Al_2O_3/antifreeze nanofluids using response surface methodology. Journal of Molecular Liquids, **261**, 14–20 (2018).

[18] H. Maddah, R. Aghayari, M. Mirzaee, M.H. Ahmadi, M. Sadeghzadeh and A.J. Chamkha, Factorial experimental design for the thermal performance of a double pipe heat exchanger using Al_2O_3–TiO_2 hybrid nanofluid. International Communications in Heat and Mass Transfer, **97**, 92–102 (2018).

[19] K. Hamid, W. Azmi, M. Nabil and R. Mamat, Improved thermal conductivity of TiO_2–SiO_2 hybrid nanofluid in ethylene glycol and water mixture. In, IOP Conference Series, Materials Science and Engineering, IOP Publishing, Vol. 1, 012067, (2017).

[20] S. Suresh, K. Venkitaraj, P. Selvakumar and M. Chandrasekar, Synthesis of Al_2O_3–Cu/water hybrid nanofluids using two step method and its thermo physical properties. Colloids and surfaces A, Physicochemical and Engineering Aspects, **388**(1–3), 41–48 (2011).

[21] T. Tayebi and A.J. Chamkha, Free convection enhancement in an annulus between horizontal confocal elliptical cylinders using hybrid nanofluids. Numerical Heat Transfer, Part A, Applications, **70**(10), 1141–1156 (2016).

[22] B.C. Pak and Y.I. Cho, Hydrodynamic and heat transfer study of dispersed fluids with submicron metallic oxide particles. Experimental Heat Transfer an International Journal, **11**(2), 151–170 (1998).

[23] Y. Xuan and W. Roetzel, Conceptions for heat transfer correlation of nanofluids. International Journal of heat and Mass transfer, **43**(19), 3701–3707 (2000).
[24] H.E. Patel, K. Anoop, T. Sundararajan and S.K. Das, A micro-convection model for thermal conductivity of nanofluids. In, International Heat Transfer Conference, Begel House Inc., 13 (2006).
[25] D.Q. Kern, Process heat transfer. Tata McGraw-Hill Education, (1950)
[26] W. Azmi, K. Sharma, P. Sarma, R. Mamat, S. Anuar and V.D. Rao, Experimental determination of turbulent forced convection heat transfer and friction factor with SiO_2 nanofluid. Experimental Thermal and Fluid Science, **51**, 103–111 (2013).
[27] E.N. Sieder and G.E. Tate, Heat transfer and pressure drop of liquids in tubes. Industrial & Engineering Chemistry, **28**(12), 1429–1435 (1936).
[28] A.M. Hussein, R.A. Bakar, K. Kadirgama and K. Sharma, Heat transfer enhancement using nanofluids in an automotive cooling system. International Communications in Heat and Mass Transfer, **53**, 195–202 (2014).
[29] A.A. Minea, Hybrid nanofluids based on Al_2O3, TiO_2 and SiO_2, numerical evaluation of different approaches. International Journal of Heat and Mass Transfer, **104**, 852–860 (2017).
[30] M.H. Esfe and M.H. Hajmohammad, Thermal conductivity and viscosity optimization of nanodiamond-Co_3O_4/EG (40, 60) aqueous nanofluid using NSGA-II coupled with RSM. Journal of Molecular Liquids, **238**, 545–552 (2017).
[31] C. Lee and K.-H. Shin, A mathematical model to predict surface roughness and pattern thickness in roll-to-roll gravure printed electronics. Robotics and Computer-Integrated Manufacturing, **29**(4), 26–32 (2013).
[32] M. Afrand, Experimental study on thermal conductivity of ethylene glycol containing hybrid nano-additives and development of a new correlation. Applied Thermal Engineering, **110**, 1111–1119 (2017).
[33] E.J. Park, S.W. Lee, I.C. Bang and H.W. Park, Optimal synthesis and characterization of Ag nanofluids by electrical explosion of wires in liquids. Nanoscale research letters, **6**(1), 223 (2011).
[34] R.H. Myers and R.H. Myers, Classical and modern regression with applications, vol. 2. Duxbury press Belmont, CA, (1990)
[35] M.H. Esfe, H. Rostamian, A. Shabani-Samghabadi and A.A.A. Arani, Application of three-level general factorial design approach for thermal conductivity of MgO/water nanofluids. Applied Thermal Engineering, **127**, 1194–1199 (2017).
[36] S. Prabhu and B.K. Vinayagam, AFM investigation in grinding process with nanofluids using Taguchi analysis. The International Journal of Advanced Manufacturing Technology, **60**(1–4), 149–160 (2012).
[37] Kazemi-Beydokhti, A., H.A. Namaghi and S.Z. Heris, Identification of the key variables on thermal conductivity of CuO nanofluid by a fractional factorial design approach. Numerical Heat Transfer, Part B, Fundamentals, **64**(6), 480–495 (2013).
[38] M.H. Esfe, S. Saedodin, M. Biglari and H. Rostamian, Experimental investigation of thermal conductivity of CNTs-Al_2O_3/water, a statistical approach. International Communications in Heat and Mass Transfer, **69**, 29–33 (2015).

Nesakumar Dharmakkan received the Bachelor degree in Chemical Engineering from Bharathiar University, Coimbatore in the year 2003 and Master degree in Chemical Engineering from Anna University, Chennai in the year 2010. He has been in the teaching field from 2010. Since 2010, he is working as Assistant Professor in the Department of Chemical Engineering at Kongu Engineering College, Perundurai, Erode, Tamilnadu, India. His research interest in the fields of Heat transfer studies and Nanotechnology.

Baskar Rajoo obtained his Bachelor's degree in Chemical Engineering from Bharathiar University and his Master's degree (Plant Design) and Doctorate from NIT, Tiruchirappalli. He has been in the teaching field from 2000. Since 2014, he is working as Professor and Head, Department of Food Technology at Kongu Engineering College, Perundurai, Erode, Tamilnadu, India. He has published about 80 research papers in national / international conferences/ journals and carried out many consultancy projects. He co-authored a book and two book chapters. He is currently handling Research projects worth of Rs. 59.5 lakhs. He produced five Ph.D., and guided ten M.E./M.Tech candidates and 09 candidates are pursuing Ph.D. under his guidance. His area of research in the field of Environmental Engineering, Heat and Mass Transfer and Bioprocess Engineering.